JOURNAL OF VIROLOGY, Mar. 2006, p. 2326–2336 Vol. 80, No. 5
0022-538X/06/$08.00+0 doi:10.1128/JVI.80.5.2326–2336.2006

Glycosylation of the Severe Acute Respiratory Syndrome Coronavirus Triple-Spanning Membrane Proteins 3a and M

M. Oostra, C. A. M. de Haan, R. J. de Groot, and P. J. M. Rottier*

Virology Division, Department of Infectious Diseases and Immunology, Utrecht University, 3584 CL Utrecht, The Netherlands

Received 6 September 2005/Accepted 8 December 2005

The severe acute respiratory syndrome coronavirus (SARS-CoV) open reading frame 3a protein has recently been shown to be a structural protein. The protein is encoded by one of the so-called group-specific genes and has no sequence homology with any of the known structural or group-specific proteins of coronaviruses. It does, however, have several similarities to the coronavirus M proteins; (i) they are triple membrane spanning with the same topology, (ii) they have similar intracellular localizations (predominantly Golgi), (iii) both are viral structural proteins, and (iv) they appear to interact with the E and S proteins, as well as with each other. The M protein plays a crucial role in coronavirus assembly and is glycosylated in all coronaviruses, either by N-linked or by O-linked oligosaccharides. The conserved glycosylation of the coronavirus M proteins and the resemblance of the 3a protein to them led us to investigate the glycosylation of these two SARS-CoV membrane proteins. The proteins were expressed separately using the vaccinia virus T7 expression system, followed by metabolic labeling. Pulse-chase analysis showed that both proteins were modified, although in different ways. While the M protein acquired cotranslationally oligosaccharides that could be removed by PNGaseF, the 3a protein acquired its modifications posttranslationally, and they were not sensitive to the *N*-glycosidase enzyme. The SARS-CoV 3a protein, however, was demonstrated to contain sialic acids, indicating the presence of oligosaccharides. O-glycosylation of the 3a protein was indeed confirmed using an in situ O-glycosylation assay of endoplasmic reticulum-retained mutants. In addition, we showed that substitution of serine and threonine residues in the ectodomain of the 3a protein abolished the addition of the O-linked sugars. Thus, the SARS-CoV 3a protein is an O-glycosylated glycoprotein, like the group 2 coronavirus M proteins but unlike the SARS-CoV M protein, which is N glycosylated.

Severe acute respiratory syndrome (SARS) recently emerged as a new human disease. It originated in southern China at the end of 2002 and spread to various areas all over the world, affecting more than 8,000 people worldwide and killing more than 800. The causative agent of the disease was rapidly identified and found to be a novel coronavirus, called SARS coronavirus (SARS-CoV) (13, 28, 39). Until then, only two human coronaviruses (HCoV) were known, 229E and OC43, both causing common colds. Since the SARS outbreak, two new human coronaviruses have been identified, HCoV-NL63 (16, 58) and HCoV-HKU1 (64), both causing potentially severe respiratory infections.

The approximately 30-kb positive-strand RNA of the SARS-CoV, fully sequenced within months after the outbreak (34, 40), appeared to have a genomic composition somewhat different from those of all known coronaviruses. All the typical coronaviral genes were readily identified among the 14 potential open reading frames (ORFs). The 5′ two-thirds of the genome is occupied by ORFs 1a and 1b, which encode the proteins involved in RNA replication and transcription. Downstream of these are the ORFs that encode the four structural proteins: the spike (S) glycoprotein, the membrane (M) protein, the envelope (E) protein, and the nucleocapsid (N) protein. However, an unusually high number (eight) of so-called group-specific genes were found interspersed between the genes in the 3′ part of the genome. By their number, nature, and location the group-specific genes differ greatly from those of other coronaviruses, placing the SARS-CoV in a distinct taxonomic position (34, 40, 50).

The group-specific genes have so far appeared not to be essential for the replication of coronaviruses, at least in cell culture. They are, however, of key importance for virus-host interactions, contributing critically to viral virulence and pathogenesis. Deletion of some or all of the group-specific genes was shown to be attenuating in the natural host for the murine hepatitis virus (MHV) (8), transmissible gastroenteritis virus (38), and feline infectious peritonitis virus (20). The SARS-CoV contains eight group-specific genes, two occurring between the S and E genes (ORFs 3a and 3b), five between the M and N genes (ORFs 6, 7a, 7b, 8a, and 8b), and one within the N gene (ORF 9b). For two of these, ORFs 3a and 7a, expression during SARS-CoV infection has been demonstrated (53, 65, 66).

With 274 amino acids, the 3a protein is the largest of the group-specific gene products. Antibodies against this protein were found in sera from convalescent SARS patients and experimentally infected animals (19, 52, 65). Hydrophobicity analysis predicts the occurrence of three transmembrane domains within the 3a protein (http://www.cbs.dtu.dk/services/TMHMM). The protein was shown to have an N-terminal ectodomain and a C-terminal endodomain (53), suggesting a membrane structure quite similar to that of the coronaviral M protein. This similarity also holds in part for the intracellular localization, as the 3a protein was found to localize in the Golgi compartment and at the cell surface, from which it is endocytosed (53, 65). The M proteins of different coronaviruses are

* Corresponding author. Mailing address: Virology Division, Department of Infectious Diseases and Immunology, Utrecht University, 3584 CL Utrecht, The Netherlands. Phone: 31 30 253 2462. Fax: 31 30 253 6723. E-mail: p.j.m.rottier@vet.uu.nl.

also primarily localized in the Golgi compartment (23, 33, 45), close to the site where coronavirus assembly takes place, i.e., in the endoplasmic reticulum (ER)-Golgi intermediate compartment (27, 54–56). Considering all these similarities to the M protein, the SARS-CoV 3a protein appeared to be a potential structural protein, which it was in fact recently demonstrated to be (26, 49).

The M proteins of all known coronaviruses are glycosylated; N-linked glycosylation and O-linked glycosylation both occur. The M proteins of group 1 and 3 coronaviruses, represented by transmissible gastroenteritis virus and infectious bronchitis virus, respectively, are only N glycosylated, i.e., they carry their oligosaccharide side chains through N linkage to asparagine residues. In contrast, M proteins of the group 2 coronaviruses, with MHV as the prototype, are only O glycosylated, thus having their side chains attached by O linkage to hydroxyl groups of serine and threonine residues (9, 24, 37, 43, 44). Many different functions have been assigned to oligosaccharide side chains. The carbohydrates have been shown to be important for folding, structure, stability, and intracellular sorting of proteins and to play a role in the generation of immune responses (12, 21, 48, 57). Glycosylation of viral glycoproteins in particular has been shown to be important for the generation of their bioactive conformation and can have effects on receptor binding, fusion activity, and antigenic properties of the virus (1, 4, 6, 62).

In the present study, the glycosylation status of the SARS-CoV M and 3a proteins was examined. The SARS-CoV M protein is predicted to be N glycosylated. For the 3a protein, the glycosylation state is of particular interest due to the protein's structural nature, its structural similarities to the M protein, and its apparent but unidentified modification(s), as observed in published work (26, 49, 53, 65, 66). The protein contains an N-glycosylation consensus sequence in its amino-terminal ectodomain. By using a number of approaches, it was established that the two proteins are indeed both glycosylated, but differently.

MATERIALS AND METHODS

Cells, viruses, and antibodies. Ost-7 cells obtained from B. Moss (14) were maintained as monolayer cultures in Dulbecco's modified Eagle's medium (Cambrex Bio Science Verviers, Belgium) containing 10% fetal calf serum (Bodinco B.V.), 100 IU of penicillin, and 100 μg of streptomycin per ml. Recombinant vaccinia virus encoding the bacteriophage T7 RNA polymerase (vTF7-3) was obtained from B. Moss (17). The polyclonal rabbit antisera directed against the SARS-CoV M and 3a proteins were obtained from Y.-J. Tan (53), and the polyclonal rabbit MHV-A59 antiserum (K134) was described earlier (44).

Plasmid constructions. All expression vectors contained the genes under control of bacteriophage T7 transcription-regulatory elements, and all SARS-CoV sequences were from isolate 5688 (29). Expression construct $pTugM_s$ contains the SARS-CoV M gene cloned in plasmid pTUG31. The SARS-CoV M gene was amplified by PCR from a construct containing the 3′-end genomic cDNA of the SARS-CoV, with primers 2054 (5′-CGAATTCGCCGCCATGGCAG ACAACGGTACTA-3′, corresponding to nucleotides 26398 to 26416 of the SARS-CoV) and 2057 (5′-CGGGATCCTTACTGTACTAGCAAAGC-3′, corresponding to nucleotides 27063 to 27046 of the SARS-CoV). Both primers contain a 5′ extension introducing EcoRI and BamHI restriction enzyme recognition sites (underlined). The PCR product was digested with EcoRI and BamHI and ligated into the EcoRI-BamHI-digested pTUG31 vector. The nucleotide sequence of the PCR product was confirmed by sequencing.

Expression construct pTug3a contains the SARS-CoV strain 5688 3a gene cloned in pTUG31. The SARS-CoV 3a gene was amplified by PCR with primers 2161 (5′-CGAGATCTACCATGGATTTGTTTATGAGA-3′, corresponding to nucleotides 25268 to 25286 of the SARS-CoV) and 2162 (5′-CGAGATCTGA ATTCTTACAAGGCACGCTAGT-3′, corresponding to nucleotides 26092 to 26074 of the SARS-CoV). Both primers contain a 5′ extension introducing a BglII restriction enzyme recognition site (underlined). The PCR product was digested with BglII and ligated into the BamHI-digested pTUG31 vector. The nucleotide sequence of the PCR product was confirmed by sequencing.

A mutant SARS-CoV 3a gene encoding a 3a protein with an ER retention signal in its carboxyl terminus was made by PCR mutagenesis using primers 2161 and 2416 (5′-AGATCTTA*GGCTGTCTTCTT*CAAAGGCACGCTAGTAGT-3′, corresponding to nucleotides 26089 to 26072 of the SARS-CoV), containing a BglII site (underlined) and the desired mutation (italics). The resulting mutant 3a gene (3aKK) was transferred as a BglII fragment into the BamHI site of expression vector pTUG31 and designated pTug3aKK.

The $pTugM_m$ and $pTugM_mKK$ expression vectors have been described previously (9, 45) and were used for the generation of the SARS-CoV 3a/MHV M hybrid expression vectors. The region encoding the SARS-CoV 3a ectodomain was amplified by PCR with primer 2454 (5′-CGCTCGAGACCATGGATTTG TTTATGAGA-3′, corresponding to nucleotides 25268 to 25286 of the SARS-CoV) containing an XhoI site (underlined) and primer 2455 (5′-TGCTTAAG GAAAGGGAGTGAGGCT-3′, corresponding to nucleotides 25397 to 25382 of the SARS-CoV) containing an AflII site. The PCR fragment was digested with XhoI and AflII and cloned into the $pTugM_m$ and $pTugM_mKK$ vectors that had been treated with the same enzymes, creating $pTug3aM_m$ and $pTug3aM_mKK$, respectively. The generation of the expression vectors for the ER-retained GalNAc transferases and sialyltransferase have been described previously (9, 41).

Mutations of the potential glycosylation sites in the SARS-CoV 3a ectodomain were introduced by PCR-based site-directed mutagenesis. Fragment 1 was amplified by PCR with primers 2454 and 2574 (5′-GC**G**G**C**C**G**CATGAACAG**C**A C**C**TG-3′, corresponding to nucleotides 25365 to 25344 of the SARS-CoV) containing a NotI site (underlined) created by the mutations (shown in boldface), while fragment 2 was amplified by PCR with primer 2573 (5′-TTCATGC**G**G**C**C GCA**G**CGATA-3′, corresponding to nucleotides 25353 to 25372 of the SARS-CoV), containing a NotI site (underlined) created by the mutation (shown in boldface), and primer 2162 containing an EcoRI site. The PCR fragments were digested with NotI and either XhoI or EcoRI and cloned by three-point ligation into the XhoI- and EcoRI-digested pTUG31 vector, creating $pTug3a^{GAAA}$. The sequences of mutated PCR products were confirmed by sequencing.

Infection and transfection. Subconfluent monolayers of Ost-7 cells grown in 10-cm^2 tissue culture dishes were inoculated with vTF7-3 at a multiplicity of infection of 10 for 1 h, after which the medium was replaced by transfection mixture, consisting of 0.5 ml of Dulbecco's modified Eagle's medium without fetal calf serum but containing 10 μl of Lipofectin (Life Technologies) and 5 μg of each selected construct. After a 5-min incubation at room temperature, 0.5 ml of Dulbecco's modified Eagle's medium was added and incubation was continued at 37°C. Three hours after infection, the medium was replaced by culture medium, and where indicated, tunicamycin (5 μg/ml) or brefeldin A (6 μg/ml) was added to the medium.

Metabolic labeling and immunoprecipitation. At 4.5 h postinfection (p.i.), the cells were starved for 30 min in cysteine- and methionine-free modified Eagle's medium containing 10 mM HEPES (pH 7.2) and 5% dialyzed fetal calf serum. The medium was then replaced by 1 ml of similar medium containing 100 μCi of ^{35}S in vitro cell-labeling mixture (Amersham), after which the cells were further incubated for the indicated time periods. When pulse-chase experiments were carried out, after the labeling period, the cells were washed once with culture medium containing 2 mM each of unlabeled methionine and cysteine and incubated further in the same medium. After the labeling or the chase, the cells were washed once with phosphate-buffered saline (PBS) containing 50 mM Ca^{2+} and 50 mM Mg^{2+} and then lysed on ice in 1 ml of lysis buffer (0.5 mM Tris [pH 7.3], 1 mM EDTA, 0.1 M NaCl, 1% Triton X-100) per 10-cm^2 dish. The lysates were cleared by centrifugation for 5 min at 15,000 rpm and 4°C.

Radioimmunoprecipitation was performed on 150- or 200-μl aliquots of lysates diluted to 1 ml with detergent buffer (50 mM Tris [pH 8.0], 62.5 mM EDTA, 1% NP-40, 0.4% sodium deoxycholate [NaDOC], 0.1% sodium dodecyl sulfate [SDS]) and antibodies (2 μl of rabbit anti-MHV serum K134 or rabbit anti-SARS-CoV M serum or 1 μl of rabbit anti-SARS-CoV 3a serum). The precipitation reaction mixtures were incubated overnight at 4°C. The immune complexes were adsorbed to Pansorbin cells (Calbiochem) for 60 min at 4°C and were subsequently collected by centrifugation. The pellets were washed three times by resuspension and centrifugation using RIPA buffer (10 mM Tris [pH 7.4], 150 mM NaCl, 0.1% SDS, 1% NP-40, 1% NaDOC). The final pellets were suspended in Laemmli sample buffer (LSB) and heated at 95°C for 5 min for the SARS-CoV 3a proteins and 1 min for the M and hybrid proteins before analysis by SDS-polyacrylamide gel electrophoresis (PAGE) using a 15% polyacrylamide gel.

Some immunoprecipitates were treated with peptide-*N*-glycosidase F (PNGaseF) (New England Biolabs), neuraminidase (arthrobacter; Roche Applied Science), or *O*-glycosidase (Roche Applied Science). In those cases, the final precipitation pellets were suspended in PBS instead of LSB and heated at 95°C, after which 2 μl PNGaseF, 2 μl neuraminidase, or 4 μl *O*-glycosidase was added and the samples were incubated overnight at 37°C; or 2 μl neuraminidase was added, and the samples were incubated at 37°C for 3 h, after which 4 μl *O*-glycosidase was added and the mixture was further incubated overnight at 37°C. Before analysis by SDS-PAGE, 0.5 volume of a three-times-concentrated solution of LSB was added to the samples.

Immunofluorescence microscopy. Ost-7 cells grown on 10-mm glass coverslips were infected with vTF7-3 at a multiplicity of infection of 10 and transfected with the different constructs. Then, 5 mM hydroxyurea (Sigma-Aldrich) was added to the medium to limit the cytopathic effect of the vaccinia virus infection. At 6 h p.i., the cells were either fixed or 5 mM cycloheximide (Sigma-Aldrich) was added to the medium and the cells were fixed 1 h later. Fixation was carried out by first washing the cells once with PBS containing 50 mM Ca^{2+} and 50 mM Mg^{2+} and then incubating them with ice-cold methanol at −20°C for 10 min. The fixed cells were washed twice with PBS and incubated for 15 min in blocking buffer (PBS-10% normal goat serum), followed by a 45-min incubation with SARS-CoV 3a antiserum diluted 1/500 in blocking buffer, MHV antiserum (K134) diluted 1/400 in blocking buffer, or mouse monoclonal anti-p58 antibody (Sigma-Aldrich) diluted 1/50 in blocking buffer. After three washes with PBS–0.05% Tween-20, the cells were stained for 45 min with fluorescein isothiocyanate-conjugated goat anti-rabbit immunoglobulin G antibodies (ICN) diluted 1/150 in blocking buffer or with Cy5-conjugated donkey anti-mouse immunoglobulin G antibodies (Jackson Laboratories) diluted 1/200 in blocking buffer. Following three washes with PBS–0.05% Tween-20 and one with PBS, the samples were mounted on glass slides in FluorSave (Calbiochem). The samples were examined with a confocal fluorescence microscope (Leica TCS SP2).

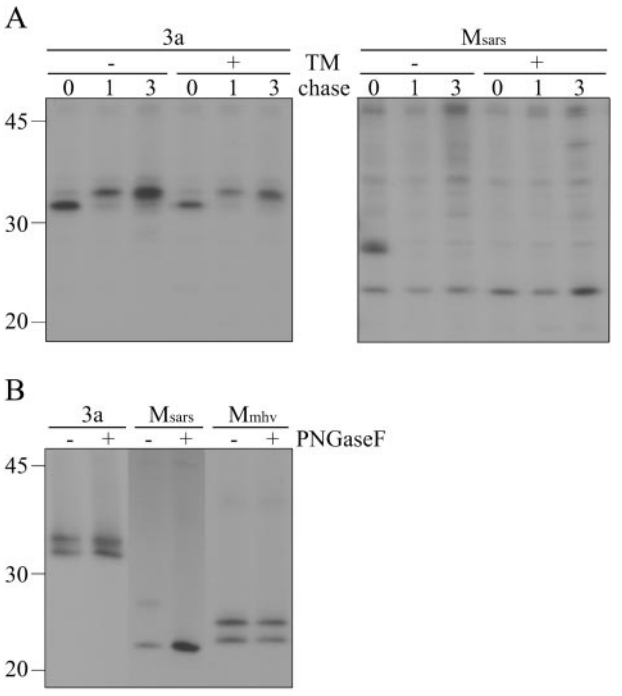

FIG. 1. Posttranslational modification of the SARS-CoV 3a protein. Recombinant vaccinia virus vTF7-3-infected Ost-7 cells were transfected with a plasmid containing the SARS-CoV 3a or M gene or the MHV M gene. The cells were labeled for 15 (A) or 60 (B) min with [^{35}S]methionine and [^{35}S]cysteine and lysed directly (A, lanes 0, and B) or chased for 1 or 3 h (A, lanes 1 and 3). The cell lysates were processed for immunoprecipitation with rabbit antisera against the SARS-CoV 3a or M protein or against MHV, followed by SDS-15% PAGE. (A) Genes were expressed in the absence (−) or presence (+) of tunicamycin (TM). (B) Half of the precipitated protein was treated with PNGaseF (+), and the other half remained untreated (−). The numbers at the left indicate the positions in the same gel of a low-molecular-weight protein marker. Only the relevant portions of the gels are shown.

RESULTS

Co- and posttranslational modifications of the SARS-CoV M and 3a proteins. To investigate whether the SARS-CoV 3a protein undergoes a posttranslational modification, a classical pulse-chase analysis was performed after the gene was expressed using the vaccinia virus vTF7-3 expression system. Ost-7 cells were infected with vTF7-3, transfected with the 3a gene-containing plasmid, pulse-labeled with [^{35}S]methionine and [^{35}S]cysteine for 15 min starting at 4.5 h p.i., and chased for 0, 1, or 3 h, followed by lysis of the cells and immunoprecipitation with a rabbit peptide antiserum directed to the endodomain (residues 134 to 274) of the 3a protein. As shown in Fig. 1A (left), the pulse-labeled product appeared as an approximately 31-kDa protein, which corresponds to the predicted size of the unmodified 3a protein. After 1 h of chase, the protein had been converted almost completely into a slower-migrating form, which had become even more prominent after 3 h of chase, during which time no additional forms had appeared. This slower-migrating form has an apparent molecular mass about 2 kDa larger than that of the unmodified 3a protein. The results indicate that the SARS-CoV 3a protein is modified posttranslationally.

To study the nature of the observed modification further, the 3a protein was expressed similarly but in the presence of tunicamycin, a drug known to prevent N glycosylation. The SARS-CoV M protein, predicted to be N glycosylated, was also included in the experiment. After the labeling, the proteins were analyzed as before, except that the immunoprecipitation of the M protein was performed with a rabbit peptide antiserum against the endodomain of this protein. As the autoradiograph in Fig. 1A (right) shows, the M protein synthesized in the absence of tunicamycin appeared as two species after pulse-labeling, the slowest migrating of which had disappeared during the chase, probably resulting from the extensive posttranslational modifications of the N-glycans in the Golgi compartment, which make the protein appear as a smear higher in the gel rather than a clear band. In the presence of the drug, the slowest-migrating species had not been formed, either during the pulse or after the chase. These observations indicate that the SARS-CoV M protein is cotranslationally modified, though incompletely, while the sensitivity to tunicamycin indicates that the modification indeed involves N glycosylation. Tunicamycin, however, did not affect the modification of the SARS-CoV 3a protein. The same protein patterns appeared as in the absence of the compound (Fig. 1A, left). Apparently, the SARS-CoV 3a protein is not modified by N glycosylation.

Further support for these conclusions was sought by studying the sensitivities of the modifications to PNGaseF, an enzyme able to specifically remove N-linked oligosaccharides from proteins. The two proteins were again expressed, radiolabeled for 1 h, and subjected to immunoprecipitation using the appropriate antibodies. The MHV M protein, known to be O glycosylated, was taken along as a control. The immunoprecipitates were split in two, and one part was treated with PNGaseF while the other was mock treated. The results, shown in Fig. 1B, revealed that the enzyme was able to remove the modi-

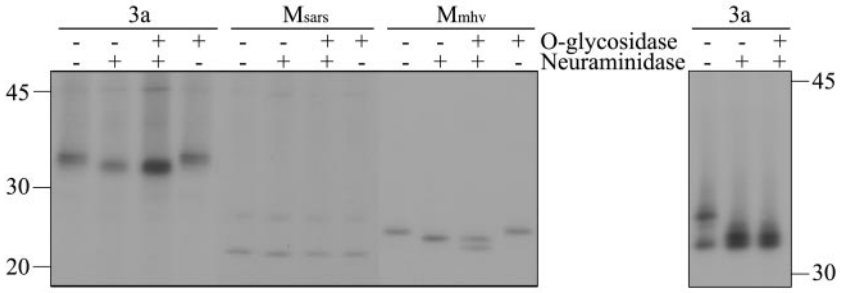

FIG. 2. Effects of neuraminidase and *O*-glycosidase on processing of the SARS-CoV 3a protein. Genes were expressed as described in the legend to Fig. 1, except that the labeling was for 60 min without chase for the SARS-CoV M protein but with 60 min of chase for the SARS-CoV 3a and MHV M proteins. The precipitated proteins were either not treated, treated with neuraminidase, treated with neuraminidase followed by treatment with *O*-glycosidase, or treated with *O*-glycosidase only. On the right, a similar analysis of the 3a protein is shown, but after electrophoresis in a longer gel. The numbers at the left and right indicate the positions in the same gel of a low-molecular-weight protein marker. Only the relevant portions of the gels are shown.

fication of the SARS-CoV M protein, thereby generating a protein that comigrated with the unmodified M species, consistent with N glycosylation. The relatively high intensity of this deglycosylated polypeptide compared to those of the mock-treated forms suggests that glycosylation of the M protein under the conditions tested gives rise to a heterogeneous collection of glycoproteins differing in their extents of oligosaccharide maturation. Hence, this diffusely migrating material becomes visible only after removal of the sugars. Unlike the M protein, the SARS-CoV 3a protein was unaffected by the PNGaseF treatment; both the primary product and its modified form appeared to be insensitive to the enzyme, as are the different forms of the control protein, MHV M. These results further support the conclusion, drawn from the observed indifference to tunicamycin, that the SARS-CoV 3a protein is not N glycosylated.

The electrophoretic mobility difference between the two forms of the SARS-CoV 3a protein resembles that of the unmodified and O-glycosylated MHV M protein. Therefore, the nature of the modification was further investigated by studying the effects of neuraminidase and *O*-glycosidase treatments on the modified proteins. *O*-Glycosidase releases the Gal β(1–3)GalNAc unit from O-glycans, but only after sialic acids have been removed. The SARS-CoV 3a and MHV M proteins were expressed, radiolabeled for 1 h, and chased for 1 h to allow oligosaccharide maturation. In parallel, the SARS-CoV M protein was expressed and labeled for 1 h without chase to limit the heterogeneous maturation. The labeled proteins were immunoprecipitated with the appropriate antibodies and treated (i) with neuraminidase only, (ii) with neuraminidase followed by *O*-glycosidase, or (iii) with *O*-glycosidase only or (iv) they were mock treated. As expected, the immature N-glycosylated form of the SARS-CoV M protein was not affected by any of the treatments (Fig. 2). In contrast, the modified forms both of the SARS-CoV 3a protein and of the MHV M protein appeared to be sensitive to neuraminidase, giving rise to species with increased mobility but still migrating slightly more slowly than the unmodified forms. While *O*-glycosidase treatment alone had no effect on either of the two proteins, when preceded by neuraminidase treatment, it did release—though not very efficiently—the O-glycans from the MHV M protein, resulting in a species that migrated with the same mobility as the unmodified MHV M protein obtained after the pulse-labeling (Fig. 1B). This combination of enzymes, however, did not seem to affect the SARS-CoV 3a protein any more than did neuraminidase alone. These results indicate that the SARS-CoV 3a protein is O glycosylated, since it is sensitive to neuraminidase but not to tunicamycin or PNGaseF. However, O glycosylation of the 3a protein is subtly different from that of the MHV M protein.

Expression of a mutant SARS-CoV 3a protein with a C-terminal ER retention signal. O glycosylation of the MHV M protein has been shown to occur in a post-ER compartment (9, 32). To try to shed light on the observed differences in the modifications of the MHV M protein and the SARS-CoV 3a protein, we investigated whether the posttranslational modification of the 3a protein also occurs after the protein has left the ER. To this end, a 3a mutant was constructed in which the gene was extended 3′ terminally with a sequence encoding the KKTA ER retention signal that proved to be effective in retaining the MHV M protein (9).

The mutant protein, named 3aKK, was expressed in parallel with the wild-type SARS-CoV 3a protein, pulse-labeled for 15 min, and chased for 15, 30, 60, or 120 min, followed by immunoprecipitation with the 3a antiserum. The analysis by SDS-PAGE (Fig. 3A) shows that the modified form of the wild-type 3a protein appeared rather rapidly, already visible as a faint band after the pulse. The conversion continued swiftly thereafter and was nearly complete after 1 h. Despite its extension, the mutant 3a protein was also posttranslationally modified, though with slower kinetics. The modified form was not observed in the pulse sample and only faintly after 15 min of chase. After 1 h, when the modification of the wild-type 3a protein was nearly complete, only about half of the 3aKK protein had been converted, and after 2 h, the process was still incomplete.

The poor effect of the retention signal on the posttranslational modification of the 3a protein could have two explanations. Either the modification already occurs in the ER or the signal does not work properly in the context of this protein. The latter appeared to be the case, as was shown using immunofluorescence. Wild-type and mutant SARS-CoV 3a proteins were expressed in duplicate cultures of Ost-7 cells. At 6 h p.i., one culture was fixed while incubation of the other was con-

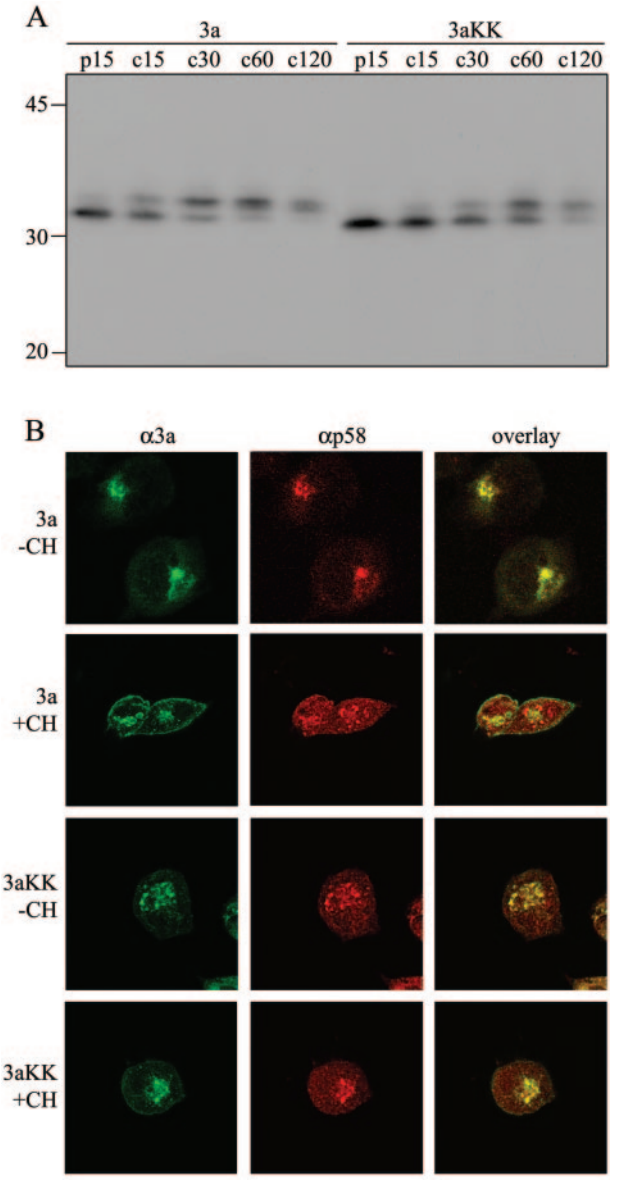

FIG. 3. Expression of a mutant SARS-CoV 3a protein with a C-terminal ER retention signal. Genes encoding wild-type SARS-CoV 3a and 3aKK were expressed in Ost-7 cells using the vTF7-3 expression system. (A) Cells were labeled for 15 min with [^{35}S]methionine and [^{35}S]cysteine and lysed directly (p15) or chased for 15, 30, 60, or 120 min. The cell lysates were processed for immunoprecipitation with an antiserum against the SARS-CoV 3a protein, followed by SDS-15% PAGE. The numbers at the left indicate the positions in the same gel of a low-molecular-weight protein marker. Only the relevant portions of the gels are shown. (B) Cells were fixed at 6 h p.i. (−CH) or cycloheximide was added at 6 h p.i. and cells were fixed 1 hour later (+CH). The cells were processed for immunofluorescence microscopy using the 3a antiserum and a monoclonal antibody against the Golgi marker p58.

tinued for an additional hour in the presence of cycloheximide to allow the synthesized proteins to reach their destinations. The cells fixed at 6 h p.i. showed typical Golgi staining for both the wild-type 3a protein and the mutant (Fig. 3B, first and third rows). Differences were observed when the cells were fixed after an additional hour in the presence of cycloheximide (second and fourth rows). While the 3aKK mutant protein apparently still had the typical Golgi localization, the wild-type 3a protein additionally showed staining of the cell surface, consistent with the fluorescence patterns observed by others (53, 65). The same results were obtained when the cells were fixed 2 hours after the addition of cycloheximide (data not shown). Clearly, the ER retention signal added to the 3a protein did not retain the protein in the ER but did restrict its localization, keeping it at an intracellular location. As a consequence, these observations still left the possibility that the posttranslational modification seen in the immunoprecipitation of the 3aKK protein is a post-ER event.

Expression of a hybrid SARS-CoV 3a/MHV M protein. The SARS-CoV 3a protein resembles coronavirus M proteins in its (putative) topology, as well as in its intracellular localization, with particular similarity to the group 2 coronavirus M proteins regarding its glycosylation. Because of this resemblance and the availability of a mutant with an effective ER retention signal (9), the MHV M protein was used to study the modification of the SARS-CoV 3a protein ectodomain. Therefore, the ectodomain of the MHV M protein was exchanged for that of the SARS-CoV 3a protein, both on the wild-type MHV M protein and on its ER-retained mutant, giving rise to two SARS-CoV 3a/MHV M hybrid proteins, one without and one carrying the ER retention signal, which were designated 3aM_m and 3aM_mKK, respectively (Fig. 4A).

The localizations of the hybrid proteins were studied by immunofluorescence and compared to those of the wild-type and ER-retained MHV M proteins (Fig. 4B). The 3aM_m hybrid protein showed typical Golgi staining that was quite similar to the staining seen for the wild-type MHV M protein, which has been demonstrated to be localized in the Golgi compartment (45). The staining seen for the hybrid protein carrying the ER retention signal, 3aM_mKK, strongly resembled the pattern of the MHV M protein with the ER retention signal, M_mKK. Both mutant proteins showed reticular staining typical of proteins localized in the ER compartment. For the mutant MHV M protein, this result is consistent with previous findings (9); for the hybrid protein, it shows that the localization of the protein is not affected by the ectodomain replacement.

Next, the posttranslational modification of the hybrid proteins was examined. The two hybrid proteins and the two MHV M proteins were again expressed, radiolabeled for 1 h, chased for 0 or 1 h, and immunoprecipitated with a polyclonal antiserum raised against purified MHV. Similar expressions and labelings were carried out in parallel in the presence of brefeldin A, a drug that recruits normally Golgi-associated proteins, including Golgi enzymes, to the ER compartment. As is clear from Fig. 4C, the 3aM_m hybrid protein was modified, the increase in mobility being similar to that seen earlier for the wild-type 3a protein. However, the progression of the 3aM_m hybrid protein to the mature form was reduced compared to both the wild-type SARS-CoV 3a protein and the wild-type MHV M protein (Fig. 4C). It is also clear that both the ER-retained MHV M protein and the hybrid protein with the ER retention signal showed no posttranslational modification at all, even when the chase was prolonged to 3 hours (data not shown). However, when brefeldin A was present during the incubations, both ER-retained proteins did obtain the post-

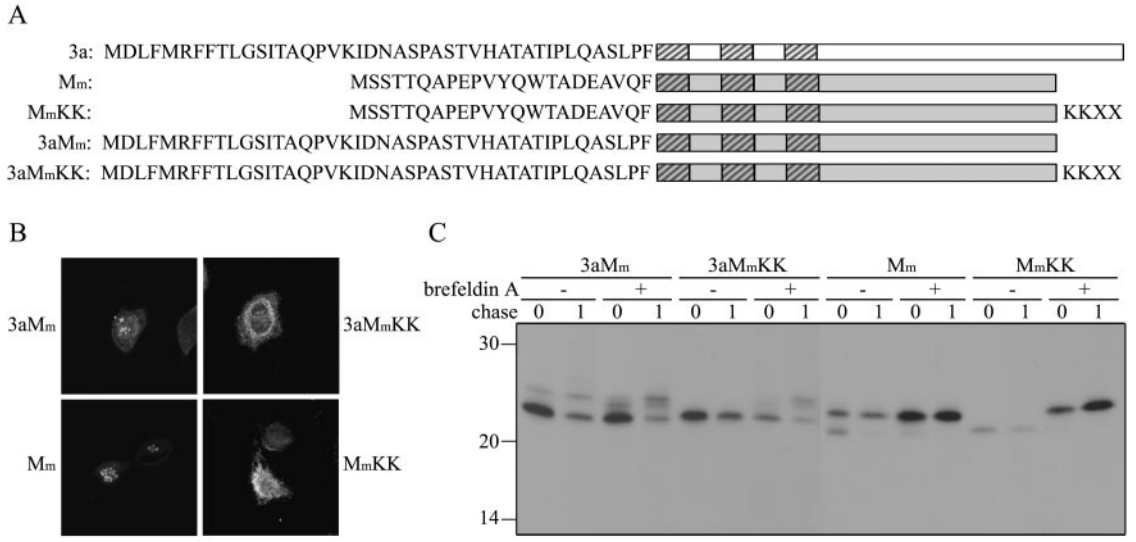

FIG. 4. Expression of a hybrid SARS-CoV 3a/MHV M protein. (A) Schematic representation of the composition of the SARS-CoV 3a/MHV M hybrid proteins. (B and C) Genes encoding the hybrid and MHV M proteins were expressed in Ost-7 cells using the vTF7-3 expression system. (B) Cycloheximide was added at 6 h p.i., and the cells were fixed 1 hour later and processed for immunofluorescence microscopy using the MHV antiserum. (C) Cells were labeled for 1 h with [^{35}S]methionine and [^{35}S]cysteine and lysed directly (0) or chased for 1 h (1). The cell lysates were processed for immunoprecipitation with polyclonal anti-MHV serum, followed by SDS-15% PAGE. The genes were expressed in the absence (−) or presence (+) of brefeldin A. The numbers at the left indicate the positions in the same gel of a low-molecular-weight protein marker. Only the relevant portions of the gels are shown.

translational modifications (Fig. 4C). The modification of the 3aM_mKK protein acquired in the presence of brefeldin A was comparable to that of the 3aM_m protein, but it was obtained somewhat faster in the presence than in the absence of brefeldin A, as was the case for the MHV M protein.

In situ glycosylation by GalNAc transferases. To provide final proof that the posttranslational modification of the SARS-CoV 3a protein is O glycosylation, an in situ O-glycosylation assay was used (9, 41). This assay is based on the coexpression of ER-resident forms of GalNAc transferases with substrates retained in the same compartment. There is no endogenous GalNAc transferase activity present in the ER, but the enzymes do function when retained (41). The ER-retained mutants of the MHV M protein and the hybrid SARS-CoV 3a/MHV M protein were expressed alone or together with the ER-retained forms of GalNAc-T1, -T2, and -T3 or with an ER-retained form of sialyltransferase used as a negative control. The proteins were pulse-labeled for 1 h and chased for 3 h, followed by immunoprecipitation with the MHV antiserum.

When coexpressed with the ER-retained sialyltransferase, both the 3aM_mKK and the M_mKK protein remained unmodified as expected (data not shown). However, when coexpressed with any of the GalNAc transferases, both proteins were converted into slower-migrating forms, indicative of GalNAc addition (Fig. 5). These modifications were most obvious with GalNac-T1 and -T3, consistent with the slower kinetics of the GalNAc-T2 enzyme observed earlier (9). While the conversion of the M_mKK protein was complete with all three enzymes, that of 3aM_mKK apparently occurred less efficiently, with the protein serving as a substrate mainly for the GalNAc-T1 enzyme, poorly for GalNAc-T3, and hardly at all for GalNAc-T2. The patterns obtained with the MHV M protein in the presence of GalNAc-T1 or -T3 actually showed two bands. This may reflect the addition of two GalNAc subunits, perhaps related to the in situ conditions, as there are no indications of double glycosylation of this protein from previous work (9, 32).

Mapping of the O-glycosylation site in the SARS-CoV 3a protein. The above-mentioned results demonstrated that the SARS-CoV 3a protein is modified by O glycosylation in its amino-terminal ectodomain. To try to localize the O-glycosylation site, the protein was analyzed using the NetOglyc3.1 software (http://www.cbs.dtu.dk/services/netoglyc). The ectodomain of the 3a protein contains nine serine and threonine residues, two of which appeared to have high O-glycosylation propensity scores (Fig. 6A). As is known from studies with the MHV M

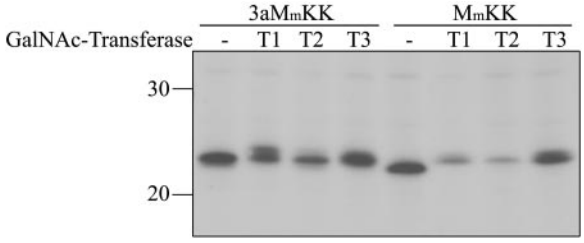

FIG. 5. Glycosylation of 3aM_mKK and M_mKK by GalNAc transferases in situ. The ER-retained hybrid or MHV M protein was expressed in Ost-7 cells using the vTF7-3 expression system, alone or in combination with ER-retained GalNAc-T1, -T2, or -T3. The cells were pulse-labeled for 1 h, followed by a 3-h chase. The cell lysates were processed for immunoprecipitation using the anti-MHV serum, followed by SDS-15% PAGE. The numbers at the left indicate the positions in the same gel of a low-molecular-weight protein marker. Only the relevant portion of the gel is shown.

A

S/T	Position	G-score	I-score	Probability
T	9	0.298	0.067	-
S	12	0.232	0.029	-
T	14	0.356	0.072	-
S	24	0.446	0.037	-
S	27	0.477	0.022	+
T	28	0.569	0.108	+++
T	32	0.512	0.319	+++
T	34	0.447	0.158	+
S	40	0.285	0.249	-

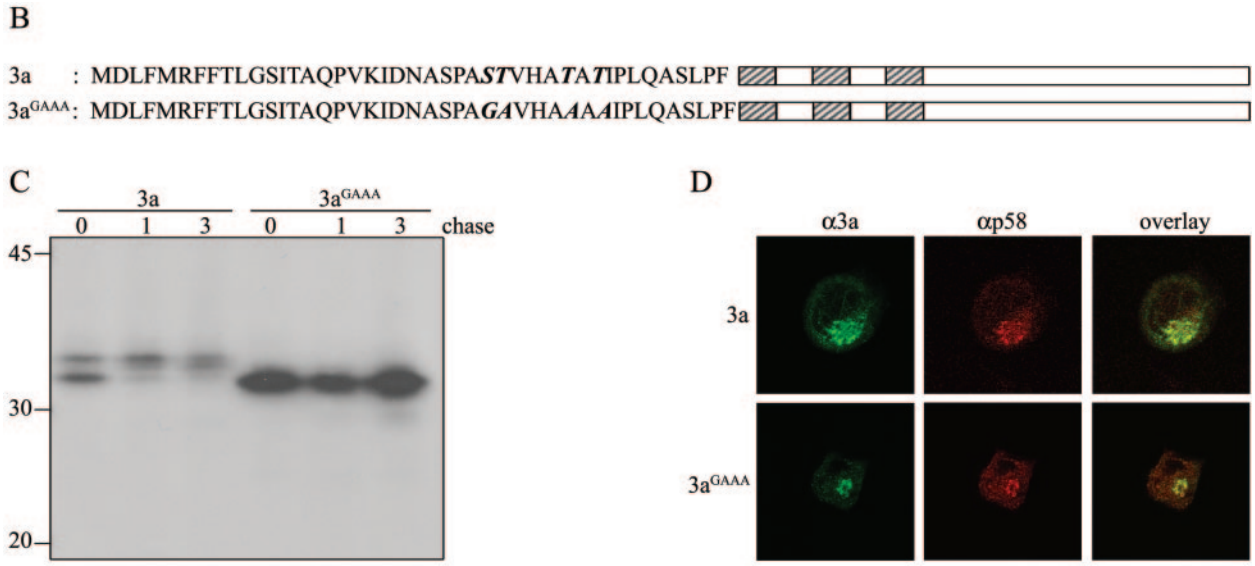

FIG. 6. Identification of the glycosylation site in the SARS-CoV 3a protein. (A) Prediction of the potential O-glycosylation site in the ectodomain of the SARS-CoV 3a protein using the NetOglyc3.1 software; the G score is the score from the general predictor, and the I score is the score from the isolated site predictor. Scores above 0.5 predict that the residue is glycosylated. −, very unlikely; +, possible; +++, likely. (B) Schematic representation of the mutations made in the ectodomain of the SARS-CoV 3a protein; changed amino acids are shown in italics. (C and D) Genes encoding the wild-type and mutated SARS-CoV 3a proteins were expressed in Ost-7 cells using the vTF7-3 expression system. (C) Cells were labeled for 1 h with [^{35}S]methionine and [^{35}S]cysteine and lysed directly (0) or chased for 1 or 3 h. The cell lysates were processed for immunoprecipitation with polyclonal anti-3a serum, followed by SDS-15% PAGE. The numbers at the left indicate the positions in the same gel of a low-molecular-weight protein marker. Only the relevant portion of the gel is shown. (D) Cells were fixed 6 h p.i. and processed for immunofluorescence microscopy using the polyclonal anti-3a serum and a monoclonal antibody against the Golgi marker p58.

protein, mutation of one glycosylation site easily leads to an alternative, not normally used acceptor site being modified instead. Therefore, it was decided to change both threonines that were predicted as likely to be glycosylated, as well as the two surrounding residues, though there are no indications of multiple glycosylation of the 3a protein. The mutations were created using PCR-based site-directed mutagenesis, the serine residue at position 27 being changed to a glycine and the threonines at positions 28, 32, and 34 to alanines (Fig. 6B).

The mutated and wild-type SARS-CoV 3a proteins were expressed, pulse-labeled for 30 min, and chased for 0, 1, or 3 h, followed by immunoprecipitation with the 3a-specific antiserum. As Fig. 6C reveals, the wild-type 3a protein was already partially glycosylated during the pulse-labeling and had become fully modified after the 1-h chase. In contrast, the mutated 3a protein had remained unmodified even after a chase of 3 hours. These observations indicated that the mutations had indeed affected the O-glycosylation site, unless they interfered with the intracellular transport of the protein, for instance, by inhibiting its ER exit. Therefore, the localizations of the wild-type and mutated 3a proteins were compared by immunofluorescence microscopy. The wild-type 3a protein showed again the typical Golgi staining seen before (Fig. 3B and 6D). This typical Golgi staining pattern was also observed for the mutated 3a protein (Fig. 6D), demonstrating that the lack of glycosylation was not caused by a change in its transport behavior. The normal transport additionally indicates that the mutations do not have a dramatic effect on the conformation of the protein and that the lack of glycosylation was probably not due to nonspecific effects of the mutations per se. It can thus be

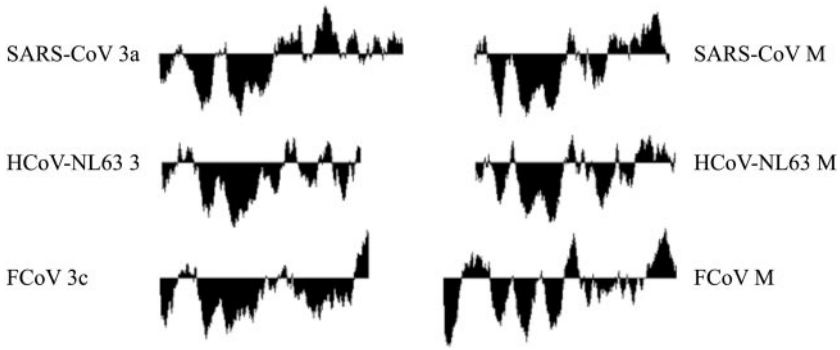

FIG. 7. Hydropathic profiles of group-specific and membrane proteins of SARS-CoV, HCoV-NL63, and feline coronavirus (FCoV). The hydropathy profiles were generated by the hydrophilicity method of Kyte-Doolittle with a window size of 17 (http://bioinformatics.weizmann.ac.il/hydroph/cmp_hydph.html).

concluded that O glycosylation of the 3a protein maps to the domain including threonines 28 and 32.

DISCUSSION

The SARS coronavirus has numerous features that set it apart from all other coronaviruses and that complicate the straightforward assignment of its taxonomic position within the coronavirus genus. One of these features is the occurrence of a second triple-spanning structural membrane protein in addition to the M protein. M proteins from the established groups of coronaviruses are known to be invariably glycosylated, either by N or by O linkage (47). The present study demonstrates the glycosylation of the SARS-CoV M and 3a proteins and allows us to conclude that triple-spanning coronaviral membrane proteins are generally glycosylated.

Though both proteins carry an N-glycosylation motif in their ectodomains, only the SARS-CoV M protein appeared to be N glycosylated. This protein thus resembles its counterparts in the group 1 and 3 coronaviruses. This is remarkable, considering the provisional grouping of the SARS-CoV among the group 2 coronaviruses (50), for which the O glycosylation of the M proteins is actually a distinguishing phenotype. The function of the glycosylation of the coronavirus M proteins is not really known. What is known is that the modification is not required for virus assembly (7, 31), nor is it critical for the interaction of the M and S proteins (10). Glycosylation is probably important for the virus in context with the host. Consistently, a study using genetically modified MHV recombinant viruses carrying M proteins that were either O glycosylated, N glycosylated, or not glycosylated at all revealed that the glycosylation state does influence the ability of the recombinant virus to replicate in the liver, but not in the brain (6). Our identification of N glycosylation as the SARS-CoV M protein's modification is in agreement with recent observations reported by Nal et al. (36). These investigators studied the biogenesis and intracellular transport of C-terminally tagged forms of the SARS-CoV S, M, and E proteins, showing that the major part of the M protein acquires complex N-linked sugars while localizing to the Golgi apparatus.

In contrast to the M protein, the SARS-CoV 3a protein appeared to be glycosylated in its ectodomain solely through O linkage, and the observed electrophoretic-mobility changes are consistent with the addition of only one oligosaccharide side chain per molecule. The primary sequence of the 3a ectodomain in fact has two hydroxyl amino acids with a high theoretical propensity for O glycosylation. Though the acceptor site actually being used was not identified, the O-glycosylation site was mapped to the region containing the predicted threonines by mutating these residues, as well as one flanking hydroxyl amino acid on either side. This region is strictly conserved in the 3a protein of the recently discovered SARS-CoV-like virus in Chinese horseshoe bats (30).

Some clear differences in the O glycosylation of the 3a protein were noticed compared to that of the MHV M protein. It appeared that the side chain added to the 3a protein in Ost-7 cells is neuraminidase sensitive but not *O*-glycosidase sensitive, in contrast to the side chain of the MHV M protein, which is both neuraminidase and *O*-glycosidase sensitive. The composition of the M protein oligosaccharide has been determined to consist of *N*-acetylgalactosamine, galactose, and sialic acids (32, 37). While the side chain of the 3a protein does contain sialic acids, as judged by its neuraminidase sensitivity, and while the protein did acquire *N*-acetylgalactosamine in the in situ glycosylation assay, it may not acquire the galactose, thereby rendering it *O*-glycosidase insensitive. Another difference from the MHV M protein was the relatively poor efficiency of modification by the different GalNAc transferases. This may have been caused by the foreign context in which the 3a ectodomain was being examined, or it may be due to the specific substrate requirements of the enzymes. More study will be required to sort out these details.

The SARS-CoV 3a protein and the coronavirus M proteins have a number of striking similarities. First of all, bioinformatics analysis predicts the SARS-CoV 3a protein to be a triple-spanning membrane protein, as has been established for coronavirus M proteins. Coronavirus M proteins have been shown to have a relatively small N-terminal ectodomain and quite a large C-terminal endodomain (2, 42, 46). This seems to hold as well for the SARS-CoV 3a protein, which was also shown to have an N-terminal ectodomain and a C-terminal endodomain (53). In fact, comparison of the hydrophobicity plots of the SARS-CoV 3a and M proteins reveals that they are markedly similar (Fig. 7) (http://bioinformatics.weizmann.ac.il/hydroph/cmp_hydph.html). Secondly, the intracellular localization of the SARS-CoV 3a protein largely coincides with that of coro-

navirus M proteins. Both are mainly found in the Golgi compartment, near the site of virus assembly (23, 27, 45, 53, 65). Thirdly, the SARS-CoV 3a protein has recently been shown to be a structural protein (26, 49), as is the coronavirus M protein. Whether the 3a protein is essential for virus assembly, as the M protein is (3, 59), remains to be established, though its dispensability for virus-like particle (VLP) formation (49) suggests that this is not the case. Finally, as this study shows, the SARS-CoV 3a protein is glycosylated, which is also a well-conserved feature of all coronavirus M proteins.

The SARS-CoV 3a protein has been shown to interact with the SARS-CoV S, E, M, and 7a proteins when coexpressed (53). Whether the glycosylation of the 3a protein is important in any of these interactions is not known. As mentioned, this modification was of no relevance for interaction of the coronavirus M proteins with other structural proteins (7, 10). While the SARS-CoV 3a protein was found to be incorporated in virions (26, 49), its role in the formation of VLPs is unclear due to the inconsistent reports about the assembly requirements for these particles. Using different systems, several groups independently showed that the expression of the SARS-CoV E and M proteins is sufficient for the formation of the VLPs (22, 35, 49), as was shown earlier for several other coronaviruses (3, 5, 18, 59). In contrast, assembly of VLPs was found by another group not to require the E protein but rather to be dependent on the N protein (25). In none of the studies was VLP formation observed to rely on the presence of the 3a protein. The protein appeared, however, to be incorporated in M/E-based particles when present, just like the S protein (49).

It is still unknown whether the 3a protein is essential for SARS-CoV replication or virion assembly and what the function(s) of the protein is. The presence of a second triple-spanning membrane protein is, so far, certainly unique among the *Coronaviridae*. This feature is, however, not unique among the *Nidovirales*, as it is common for the *Arteriviridae*, another family within this order. These viruses typically have two triple-spanning membrane proteins, M and GP_5, of which the latter is N glycosylated while the M protein remains unglycosylated. The two proteins occur in virions as heterodimers formed by disulfide bonds between conserved cysteine residues in their ectodomains (11, 15, 51, 60). The proteins are both essential for the production of viral particles (51, 61, 63).

The question might be raised as to whether the occurrence of a second triple-spanning membrane protein in the SARS-CoV is really all that unique for coronaviruses. There is a high degree of sequence variation between the coronavirus M proteins, especially between M proteins of the different coronavirus groups, but their hydropathy profiles are remarkably similar (47). This is also the case for the SARS-CoV 3a protein and the M protein. Intriguingly, when prediction programs are applied to the proteomes of other coronaviruses, it appears that all group 1 viruses express group-specific proteins predicted to be triple-spanning membrane proteins. Examples are the feline coronavirus ORF 3c protein and the HCoV-NL63 ORF 3 protein, the hydropathy profiles of which are depicted in Fig. 7, together with those of the corresponding M proteins of these viruses, in comparison with the SARS-CoV 3a and M proteins. Despite the small amount of sequence homology among these proteins, the similarities in their hydropathy profiles, both to each other and to the corresponding M proteins, as well as to the SARS-CoV 3a protein, are quite remarkable. Nothing is actually known about these proteins, but it is clear that it will be interesting to learn more about their biological features. In particular, it will be important to address questions concerning the structural natures of the proteins and their interactions with other structural proteins. In fact, such questions might be studied more conveniently with these group 1 coronaviruses than with the SARS coronavirus.

ACKNOWLEDGMENTS

We are grateful to Martijn van Beijnen for help with the initial experiments and to Yee Joo Tan for providing the SARS-CoV antisera.

REFERENCES

1. **Alexander, S., and J. H. Elder.** 1984. Carbohydrate dramatically influences immune reactivity of antisera to viral glycoprotein antigens. Science **226:** 1328–1330.
2. **Armstrong, J., H. Niemann, S. Smeekens, P. Rottier, and G. Warren.** 1984. Sequence and topology of a model intracellular membrane protein, E1 glycoprotein, from a coronavirus. Nature **308:**751–752.
3. **Baudoux, P., C. Carrat, L. Besnardeau, B. Charley, and H. Laude.** 1998. Coronavirus pseudoparticles formed with recombinant M and E proteins induce alpha interferon synthesis by leukocytes. J. Virol. **72:**8636–8643.
4. **Braakman, I., and E. van Anken.** 2000. Folding of viral envelope glycoproteins in the endoplasmic reticulum. Traffic **1:**533–539.
5. **Corse, E., and C. E. Machamer.** 2000. Infectious bronchitis virus E protein is targeted to the Golgi complex and directs release of virus-like particles. J. Virol. **74:**4319–4326.
6. **de Haan, C. A., M. de Wit, L. Kuo, C. Montalto-Morrison, B. L. Haagmans, S. R. Weiss, P. S. Masters, and P. J. Rottier.** 2003. The glycosylation status of the murine hepatitis coronavirus M protein affects the interferogenic capacity of the virus in vitro and its ability to replicate in the liver but not the brain. Virology **312:**395–406.
7. **de Haan, C. A., L. Kuo, P. S. Masters, H. Vennema, and P. J. Rottier.** 1998. Coronavirus particle assembly: primary structure requirements of the membrane protein. J. Virol. **72:**6838–6850.
8. **de Haan, C. A., P. S. Masters, X. Shen, S. Weiss, and P. J. Rottier.** 2002. The group-specific murine coronavirus genes are not essential, but their deletion, by reverse genetics, is attenuating in the natural host. Virology **296:**177–189.
9. **de Haan, C. A., P. Roestenberg, M. de Wit, A. A. de Vries, T. Nilsson, H. Vennema, and P. J. Rottier.** 1998. Structural requirements for O-glycosylation of the mouse hepatitis virus membrane protein. J. Biol. Chem. **273:** 29905–29914.
10. **de Haan, C. A., M. Smeets, F. Vernooij, H. Vennema, and P. J. Rottier.** 1999. Mapping of the coronavirus membrane protein domains involved in interaction with the spike protein. J. Virol. **73:**7441–7452.
11. **de Vries, A. A., S. M. Post, M. J. Raamsman, M. C. Horzinek, and P. J. Rottier.** 1995. The two major envelope proteins of equine arteritis virus associate into disulfide-linked heterodimers. J. Virol. **69:**4668–4674.
12. **Drickamer, K., and M. E. Taylor.** 1998. Evolving views of protein glycosylation. Trends Biochem. Sci. **23:**321–324.
13. **Drosten, C., S. Gunther, W. Preiser, S. van der Werf, H. R. Brodt, S. Becker, H. Rabenau, M. Panning, L. Kolesnikova, R. A. Fouchier, A. Berger, A. M. Burguiere, J. Cinatl, M. Eickmann, N. Escriou, K. Grywna, S. Kramme, J. C. Manuguerra, S. Muller, V. Rickerts, M. Sturmer, S. Vieth, H. D. Klenk, A. D. Osterhaus, H. Schmitz, and H. W. Doerr.** 2003. Identification of a novel coronavirus in patients with severe acute respiratory syndrome. N. Engl. J. Med. **348:**1967–1976.
14. **Elroy-Stein, O., and B. Moss.** 1990. Cytoplasmic expression system based on constitutive synthesis of bacteriophage T7 RNA polymerase in mammalian cells. Proc. Natl. Acad. Sci. USA **87:**6743–6747.
15. **Faaberg, K. S., C. Even, G. A. Palmer, and P. G. Plagemann.** 1995. Disulfide bonds between two envelope proteins of lactate dehydrogenase-elevating virus are essential for viral infectivity. J. Virol. **69:**613–617.
16. **Fouchier, R. A., N. G. Hartwig, T. M. Bestebroer, B. Niemeyer, J. C. de Jong, J. H. Simon, and A. D. Osterhaus.** 2004. A previously undescribed coronavirus associated with respiratory disease in humans. Proc. Natl. Acad. Sci. USA **101:**6212–6216.
17. **Fuerst, T. R., E. G. Niles, F. W. Studier, and B. Moss.** 1986. Eukaryotic transient-expression system based on recombinant vaccinia virus that synthesizes bacteriophage T7 RNA polymerase. Proc. Natl. Acad. Sci. USA **83:**8122–8126.
18. **Godeke, G. J., C. A. de Haan, J. W. Rossen, H. Vennema, and P. J. Rottier.** 2000. Assembly of spikes into coronavirus particles is mediated by the carboxy-terminal domain of the spike protein. J. Virol. **74:**1566–1571.
19. **Guo, J. P., M. Petric, W. Campbell, and P. L. McGeer.** 2004. SARS coronavirus peptides recognized by antibodies in the sera of convalescent cases. Virology **324:**251–256.

20. **Haijema, B. J., H. Volders, and P. J. Rottier.** 2004. Live, attenuated coronavirus vaccines through the directed deletion of group-specific genes provide protection against feline infectious peritonitis. J. Virol. **78:**3863–3871.
21. **Helenius, A., and M. Aebi.** 2001. Intracellular functions of N-linked glycans. Science **291:**2364–2369.
22. **Ho, Y., P. H. Lin, C. Y. Liu, S. P. Lee, and Y. C. Chao.** 2004. Assembly of human severe acute respiratory syndrome coronavirus-like particles. Biochem. Biophys. Res. Commun. **318:**833–838.
23. **Hogue, B. G., and D. P. Nayak.** 1990. Expression of the porcine transmissible gastroenteritis coronavirus M protein. Adv. Exp. Med. Biol. **276:**121–126.
24. **Holmes, K. V., E. W. Doller, and L. S. Sturman.** 1981. Tunicamycin resistant glycosylation of coronavirus glycoprotein: demonstration of a novel type of viral glycoprotein. Virology **115:**334–344.
25. **Huang, Y., Z. Y. Yang, W. P. Kong, and G. J. Nabel.** 2004. Generation of synthetic severe acute respiratory syndrome coronavirus pseudoparticles: implications for assembly and vaccine production. J. Virol. **78:**12557–12565.
26. **Ito, N., E. C. Mossel, K. Narayanan, V. L. Popov, C. Huang, T. Inoue, C. J. Peters, and S. Makino.** 2005. Severe acute respiratory syndrome coronavirus 3a protein is a viral structural protein. J. Virol. **79:**3182–3186.
27. **Klumperman, J., J. K. Locker, A. Meijer, M. C. Horzinek, H. J. Geuze, and P. J. Rottier.** 1994. Coronavirus M proteins accumulate in the Golgi complex beyond the site of virion budding. J. Virol. **68:**6523–6534.
28. **Ksiazek, T. G., D. Erdman, C. S. Goldsmith, S. R. Zaki, T. Peret, S. Emery, S. Tong, C. Urbani, J. A. Comer, W. Lim, P. E. Rollin, S. F. Dowell, A. E. Ling, C. D. Humphrey, W. J. Shieh, J. Guarner, C. D. Paddock, P. Rota, B. Fields, J. DeRisi, J. Y. Yang, N. Cox, J. M. Hughes, J. W. LeDuc, W. J. Bellini, and L. J. Anderson.** 2003. A novel coronavirus associated with severe acute respiratory syndrome. N. Engl. J. Med. **348:**1953–1966.
29. **Kuiken, T., R. A. Fouchier, M. Schutten, G. F. Rimmelzwaan, G. van Amerongen, D. van Riel, J. D. Laman, T. de Jong, G. van Doornum, W. Lim, A. E. Ling, P. K. Chan, J. S. Tam, M. C. Zambon, R. Gopal, C. Drosten, S. van der Werf, N. Escriou, J. C. Manuguerra, K. Stohr, J. S. Peiris, and A. D. Osterhaus.** 2003. Newly discovered coronavirus as the primary cause of severe acute respiratory syndrome. Lancet **362:**263–270.
30. **Lau, S. K., P. C. Woo, K. S. Li, Y. Huang, H. W. Tsoi, B. H. Wong, S. S. Wong, S. Y. Leung, K. H. Chan, and K. Y. Yuen.** 2005. Severe acute respiratory syndrome coronavirus-like virus in Chinese horseshoe bats. Proc. Natl. Acad. Sci. USA **102:**14040–14045.
31. **Laude, H., J. Gelfi, L. Lavenant, and B. Charley.** 1992. Single amino acid changes in the viral glycoprotein M affect induction of alpha interferon by the coronavirus transmissible gastroenteritis virus. J. Virol. **66:**743–749.
32. **Locker, J. K., G. Griffiths, M. C. Horzinek, and P. J. Rottier.** 1992. O-glycosylation of the coronavirus M protein. Differential localization of sialyltransferases in N- and O-linked glycosylation. J. Biol. Chem. **267:**14094–14101.
33. **Machamer, C. E., S. A. Mentone, J. K. Rose, and M. G. Farquhar.** 1990. The E1 glycoprotein of an avian coronavirus is targeted to the *cis* Golgi complex. Proc. Natl. Acad. Sci. USA **87:**6944–6948.
34. **Marra, M. A., S. J. Jones, C. R. Astell, R. A. Holt, A. Brooks-Wilson, Y. S. Butterfield, J. Khattra, J. K. Asano, S. A. Barber, S. Y. Chan, A. Cloutier, S. M. Coughlin, D. Freeman, N. Girn, O. L. Griffith, S. R. Leach, M. Mayo, H. McDonald, S. B. Montgomery, P. K. Pandoh, A. S. Petrescu, A. G. Robertson, J. E. Schein, A. Siddiqui, D. E. Smailus, J. M. Stott, G. S. Yang, F. Plummer, A. Andonov, H. Artsob, N. Bastien, K. Bernard, T. F. Booth, D. Bowness, M. Czub, M. Drebot, L. Fernando, R. Flick, M. Garbutt, M. Gray, A. Grolla, S. Jones, H. Feldmann, A. Meyers, A. Kabani, Y. Li, S. Normand, U. Stroher, G. A. Tipples, S. Tyler, R. Vogrig, D. Ward, B. Watson, R. C. Brunham, M. Krajden, M. Petric, D. M. Skowronski, C. Upton, and R. L. Roper.** 2003. The genome sequence of the SARS-associated coronavirus. Science **300:**1399–1404.
35. **Mortola, E., and P. Roy.** 2004. Efficient assembly and release of SARS coronavirus-like particles by a heterologous expression system. FEBS Lett. **576:**174–178.
36. **Nal, B., C. Chan, F. Kien, L. Siu, J. Tse, K. Chu, J. Kam, I. Staropoli, B. Crescenzo-Chaigne, N. Escriou, S. van der Werf, K. Y. Yuen, and R. Altmeyer.** 2005. Differential maturation and subcellular localization of severe acute respiratory syndrome coronavirus surface proteins S, M and E. J. Gen. Virol. **86:**1423–1434.
37. **Niemann, H., R. Geyer, H. D. Klenk, D. Linder, S. Stirm, and M. Wirth.** 1984. The carbohydrates of mouse hepatitis virus (MHV) A59: structures of the O-glycosidically linked oligosaccharides of glycoprotein E1. EMBO J. **3:**665–670.
38. **Ortego, J., I. Sola, F. Almazan, J. E. Ceriani, C. Riquelme, M. Balasch, J. Plana, and L. Enjuanes.** 2003. Transmissible gastroenteritis coronavirus gene 7 is not essential but influences in vivo virus replication and virulence. Virology **308:**13–22.
39. **Peiris, J. S., S. T. Lai, L. L. Poon, Y. Guan, L. Y. Yam, W. Lim, J. Nicholls, W. K. Yee, W. W. Yan, M. T. Cheung, V. C. Cheng, K. H. Chan, D. N. Tsang, R. W. Yung, T. K. Ng, and K. Y. Yuen.** 2003. Coronavirus as a possible cause of severe acute respiratory syndrome. Lancet **361:**1319–1325.
40. **Rota, P. A., M. S. Oberste, S. S. Monroe, W. A. Nix, R. Campagnoli, J. P. Icenogle, S. Penaranda, B. Bankamp, K. Maher, M. H. Chen, S. Tong, A. Tamin, L. Lowe, M. Frace, J. L. DeRisi, Q. Chen, D. Wang, D. D. Erdman, T. C. Peret, C. Burns, T. G. Ksiazek, P. E. Rollin, A. Sanchez, S. Liffick, B. Holloway, J. Limor, K. McCaustland, M. Olsen-Rasmussen, R. Fouchier, S. Gunther, A. D. Osterhaus, C. Drosten, M. A. Pallansch, L. J. Anderson, and W. J. Bellini.** 2003. Characterization of a novel coronavirus associated with severe acute respiratory syndrome. Science **300:**1394–1399.
41. **Rottger, S., J. White, H. H. Wandall, J. C. Olivo, A. Stark, E. P. Bennett, C. Whitehouse, E. G. Berger, H. Clausen, and T. Nilsson.** 1998. Localization of three human polypeptide GalNAc-transferases in HeLa cells suggests initiation of O-linked glycosylation throughout the Golgi apparatus. J. Cell Sci. **111:**45–60.
42. **Rottier, P., D. Brandenburg, J. Armstrong, B. van der Zeijst, and G. Warren.** 1984. Assembly in vitro of a spanning membrane protein of the endoplasmic reticulum: the E1 glycoprotein of coronavirus mouse hepatitis virus A59. Proc. Natl. Acad. Sci. USA **81:**1421–1425.
43. **Rottier, P. J.** 1990. Background paper. Coronavirus M and HE: two peculiar glycoproteins. Adv. Exp. Med. Biol. **276:**91–94.
44. **Rottier, P. J., M. C. Horzinek, and B. A. van der Zeijst.** 1981. Viral protein synthesis in mouse hepatitis virus strain A59-infected cells: effect of tunicamycin. J. Virol. **40:**350–357.
45. **Rottier, P. J., and J. K. Rose.** 1987. Coronavirus E1 glycoprotein expressed from cloned cDNA localizes in the Golgi region. J. Virol. **61:**2042–2045.
46. **Rottier, P. J., G. W. Welling, S. Welling-Wester, H. G. Niesters, J. A. Lenstra, and B. A. Van der Zeijst.** 1986. Predicted membrane topology of the coronavirus protein E1. Biochemistry **25:**1335–1339.
47. **Rottier, P. J. M.** 1995. The coronavirus membrane protein, p. 115–139. *In* S. G. Siddell (ed.), The Coronaviridae. Plenum Press, New York, N.Y.
48. **Rudd, P. M., and R. A. Dwek.** 1997. Glycosylation: heterogeneity and the 3D structure of proteins. Crit. Rev. Biochem. Mol. Biol. **32:**1–100.
49. **Shen, S., P. S. Lin, Y. C. Chao, A. Zhang, X. Yang, S. G. Lim, W. Hong, and Y. J. Tan.** 2005. The severe acute respiratory syndrome coronavirus 3a is a novel structural protein. Biochem. Biophys. Res. Commun. **330:**286–292.
50. **Snijder, E. J., P. J. Bredenbeek, J. C. Dobbe, V. Thiel, J. Ziebuhr, L. L. Poon, Y. Guan, M. Rozanov, W. J. Spaan, and A. E. Gorbalenya.** 2003. Unique and conserved features of genome and proteome of SARS-coronavirus, an early split-off from the coronavirus group 2 lineage. J. Mol. Biol. **331:**991–1004.
51. **Snijder, E. J., J. C. Dobbe, and W. J. Spaan.** 2003. Heterodimerization of the two major envelope proteins is essential for arterivirus infectivity. J. Virol. **77:**97–104.
52. **Tan, Y. J., P. Y. Goh, B. C. Fielding, S. Shen, C. F. Chou, J. L. Fu, H. N. Leong, Y. S. Leo, E. E. Ooi, A. E. Ling, S. G. Lim, and W. Hong.** 2004. Profiles of antibody responses against severe acute respiratory syndrome coronavirus recombinant proteins and their potential use as diagnostic markers. Clin. Diagn. Lab. Immunol. **11:**362–371.
53. **Tan, Y. J., E. Teng, S. Shen, T. H. Tan, P. Y. Goh, B. C. Fielding, E. E. Ooi, H. C. Tan, S. G. Lim, and W. Hong.** 2004. A novel severe acute respiratory syndrome coronavirus protein, U274, is transported to the cell surface and undergoes endocytosis. J. Virol. **78:**6723–6734.
54. **Tooze, J., S. Tooze, and G. Warren.** 1984. Replication of coronavirus MHV-A59 in sac− cells: determination of the first site of budding of progeny virions. Eur. J. Cell Biol. **33:**281–293.
55. **Tooze, J., and S. A. Tooze.** 1985. Infection of AtT20 murine pituitary tumour cells by mouse hepatitis virus strain A59: virus budding is restricted to the Golgi region. Eur. J. Cell Biol. **37:**203–212.
56. **Tooze, J., S. A. Tooze, and G. Warren.** 1985. Laminated cisternae of the rough endoplasmic reticulum induced by coronavirus MHV-A59 infection. Eur. J. Cell Biol. **36:**108–115.
57. **Van den Steen, P., P. M. Rudd, R. A. Dwek, and G. Opdenakker.** 1998. Concepts and principles of O-linked glycosylation. Crit. Rev. Biochem. Mol. Biol. **33:**151–208.
58. **van der Hoek, L., K. Pyrc, M. F. Jebbink, W. Vermeulen-Oost, R. J. Berkhout, K. C. Wolthers, P. M. Wertheim-van Dillen, J. Kaandorp, J. Spaargaren, and B. Berkhout.** 2004. Identification of a new human coronavirus. Nat. Med. **10:**368–373.
59. **Vennema, H., G. J. Godeke, J. W. Rossen, W. F. Voorhout, M. C. Horzinek, D. J. Opstelten, and P. J. Rottier.** 1996. Nucleocapsid-independent assembly of coronavirus-like particles by co-expression of viral envelope protein genes. EMBO J. **15:**2020–2028.
60. **Verheije, M. H.** 2002. Genetic engineering of the porcine reproductive and respiratory syndrome virus: exploration of avenues towards a vaccine. Ph.D. thesis. Utrecht University, Utrecht, The Netherlands.
61. **Wieringa, R., A. A. de Vries, J. van der Meulen, G. J. Godeke, J. J. Onderwater, H. van Tol, H. K. Koerten, A. M. Mommaas, E. J. Snijder, and P. J. Rottier.** 2004. Structural protein requirements in equine arteritis virus assembly. J. Virol. **78:**13019–13027.
62. **Wissink, E. H., M. V. Kroese, J. G. Maneschijn-Bonsing, J. J. Meulenberg, P. A. van Rijn, F. A. Rijsewijk, and P. J. Rottier.** 2004. Significance of the oligosaccharides of the porcine reproductive and respiratory syndrome virus glycoproteins GP2a and GP5 for infectious virus production. J. Gen. Virol. **85:**3715–3723.
63. **Wissink, E. H. J., M. V. Kroese, H. A. R. van Wijk, F. A. M. Rijsewijk, J. J. M. Meulenberg, and P. J. M. Rottier.** 2005. Envelope protein requirements for

the assembly of infectious virions of porcine reproductive and respiratory syndrome virus (PRRSV). J. Virol. **79:**12495–12506.

64. **Woo, P. C., S. K. Lau, C. M. Chu, K. H. Chan, H. W. Tsoi, Y. Huang, B. H. Wong, R. W. Poon, J. J. Cai, W. K. Luk, L. L. Poon, S. S. Wong, Y. Guan, J. S. Peiris, and K. Y. Yuen.** 2005. Characterization and complete genome sequence of a novel coronavirus, coronavirus HKU1, from patients with pneumonia. J. Virol. **79:**884–895.
65. **Yu, C. J., Y. C. Chen, C. H. Hsiao, T. C. Kuo, S. C. Chang, C. Y. Lu, W. C. Wei, C. H. Lee, L. M. Huang, M. F. Chang, H. N. Ho, and F. J. Lee.** 2004. Identification of a novel protein 3a from severe acute respiratory syndrome coronavirus. FEBS Lett. **565:**111–116.
66. **Zeng, R., R. F. Yang, M. D. Shi, M. R. Jiang, Y. H. Xie, H. Q. Ruan, X. S. Jiang, L. Shi, H. Zhou, L. Zhang, X. D. Wu, Y. Lin, Y. Y. Ji, L. Xiong, Y. Jin, E. H. Dai, X. Y. Wang, B. Y. Si, J. Wang, H. X. Wang, C. E. Wang, Y. H. Gan, Y. C. Li, J. T. Cao, J. P. Zuo, S. F. Shan, E. Xie, S. H. Chen, Z. Q. Jiang, X. Zhang, Y. Wang, G. Pei, B. Sun, and J. R. Wu.** 2004. Characterization of the 3a protein of SARS-associated coronavirus in infected Vero E6 cells and SARS patients. J. Mol. Biol. **341:**271–279.